Influence of embedded-carbon nanotubes on the thermal properties of copper matrix nanocomposites processed by molecular-level mixing

Kyung Tae Kim,[a,*] Jürgen Eckert,[b,c] Gang Liu,[b,1] Jin Man Park,[b] Byung Kyu Lim[d] and Soon Hyung Hong[d]

[a]Functional Materials Division, Korea Institute of Materials Science, 66 Sangnam-dong, Changwon-city, Gyeongnam 641-831, Republic of Korea
[b]IFW Dresden, Institute for Complex Materials, P.O. Box 270116, D-01171 Dresden, Germany
[c]TU Dresden, Institute of Materials Science, D-01062 Dresden, Germany
[d]Department of Materials Science and Engineering, and KAIST Institute for the NanoCentury, KAIST, 373-1 Kusung-dong Yusung-gu, Daejeon 305-701, Republic of Korea

The microstructure of carbon nanotube reinforced copper matrix (CNT/Cu) nanocomposites, processed by molecular-level mixing, exhibits CNTs homogeneously dispersed in the Cu matrix. Measured thermal conductivity of the fabricated CNT/Cu nanocomposites decreased as the CNT volume fraction increased from 5% to 10%. A low coefficient of thermal expansion (CTE) was obtained from the 10 vol.% CNT/Cu nanocomposite. These results indicate that embedded CNTs provide CNT/metal interfaces as thermal barriers but also stiffen the metal matrix composites.
© 2010 Acta Materialia Inc. Published by Elsevier Ltd. All rights reserved.

Keywords: Metal matrix composites; Nanocomposite; Carbon and graphite; Thermal conductivity

Carbon nanotubes (CNTs) have attracted much attention as fillers of various matrices, such as polymers and metals for thermal management applications, due to their extraordinarily low coefficient of thermal expansion (CTE) [1] of close to 0 ppm K^{-1} and outstanding axial thermal conductivity [2,3]. So far, most investigations on the thermal properties of materials upon CNT addition have focused on polymer matrix composites fabricated through interfacial treatment [4], purification [5] and creation of anisotropy [6] of CNTs. Compared to CNT/polymer composites, there have been only very limited reports on the thermal properties of CNT/metal composites [7–9]. For example, Tang et al. [7] reported single-walled CNT/Al composites with lower CTEs than for the Al matrix. Chu et al. [9] ana-

lyzed the effective thermal conductivity of CNT/Cu composites fabricated by powder metallurgy (PM).

Despite these efforts, direct application of CNT/metal composites to thermal management materials is still limited because of the problem of agglomeration of CNTs in the matrix caused by PM processing, which has not yet been fully solved. In order to solve this issue, we previously developed a synthesis route based on molecular-level mixing [10] that provides an extremely reduced agglomeration of CNTs within metal matrix composites. However, so far our investigations [10–12] have been mainly focused on the enhancement of the mechanical strength of the fabricated CNT/Cu nanocomposites.

Here, we synthesize CNT/Cu nanocomposites by using the molecular-level mixing process and report on their thermal properties. For comparison, pure Cu was fabricated by the same process but without CNTs. The measured thermal conductivity of the nanocomposites exhibits decreased values compared to that of unreinforced Cu. The concept of the thermal barrier effect at CNT/Cu interfaces originating from functionalized CNTs is suggested to explain this degradation in ther-

---

* Corresponding author. Tel.: +82 55 280 3506; fax: +82 55 280 3392; e-mail: ktkim@kims.re.kr
[1] Current address: State Key Laboratory for Mechanical Behavior of Materials, School of Materials Science and Engineering, Xi'an Jiaotong University, Xi'an, 710049, China.

mal conductivity of the nanocomposites. The low CTE of the composites is described by the concept of the Cu matrix stiffened by reinforcing CNTs.

In order to fabricate the present CNT/Cu nanocomposites, multi-walled CNTs were used as reinforcements. They were purified in HF solution and then functionalized in a mixed solution of H_2SO_4/HNO_3 (3:1 ratio). The functionalized CNTs were dispersed within ethanol by sonication to form a stable suspension. $Cu(CH_3COO)_2H_2O$ (Aldrich 21,755–7) was added to the CNT suspension and sonicated for 2 h. This procedure is termed "molecular-level mixing process" (for more experimental details on this process, see Ref. [10]). The solution mixed at the molecular level was vaporized at 333–373 K and subsequently calcinated at 573 K in air. The calcinated CNT/Cu oxide powders were reduced at 523 K for 4 h under hydrogen atmosphere. The CNT/Cu nanocomposite powders obtained were consolidated by spark plasma sintering at 823 K for 1 min in a vacuum of 0.13 Pa with an applied pressure of 50 MPa. The weight percentages of CNTs determined by elemental analysis (EA1110-FISONS) of the CNT/Cu composite powders were converted into volume fractions. The weight percentages of oxygen in the unreinforced Cu and the CNT/Cu nanocomposites were also characterized by elemental analysis. The CNT/Cu nanocomposites were wet-etched using a mixed solution of HCl and $Fe(NO_3)_2$ in distilled water. The microstructure was analyzed by field emission scanning electron microscopy (XL30SFEG) and high-resolution transmission electron microscopy (HRTEM; JEM3010, 300 kV), respectively. The thermal diffusivity of the unreinforced Cu and the CNT/Cu nanocomposites was characterized by the Laser Flash method (LFA 457). The CTE of the samples was measured by dilatometry (DIL402C).

A cross-sectional image of the 5 vol.% CNT/Cu nanocomposite shows the CNTs ro be uniformly dispersed rather than severely agglomerated in the Cu matrix, as shown in Figure 1a. As the weak wet-etching treatment to the nanocomposite slightly peels off the Cu materials covered in the surface, embedded CNTs are revealed. Many voids and crack-like regions can be seen around the CNTs. This means that the interfacial region near the CNTs is chemically unstable and might be different from the Cu-only region.

As shown in Table 1, excessive oxygen contents compared to unreinforced Cu are observed in CNT/Cu nanocomposites with increasing CNT volume fraction. Assuming that the oxygen atoms discovered in unreinforced Cu are distributed homogeneously throughout the whole sample, the excessive oxygen atoms must originate from the added CNTs which are chemically functionalized in the molecular-level mixing process. We previously found [11] excessive oxygen atoms caused by adding functionalized CNTs in the composite powder state.

The high-resolution TEM image of the fabricated 5 vol.% CNT/Cu nanocomposite shown in Figure 1b reveals that the CNTs are individually embedded in the Cu matrix without agglomeration. The inset in Figure 1b shows the Fourier transformed pattern from the matrix, which can be identified as the [1 1 0] zone axis of the face-centered cubic Cu phase. It is confirmed that multi-walled structures of CNTs are present in the matrix
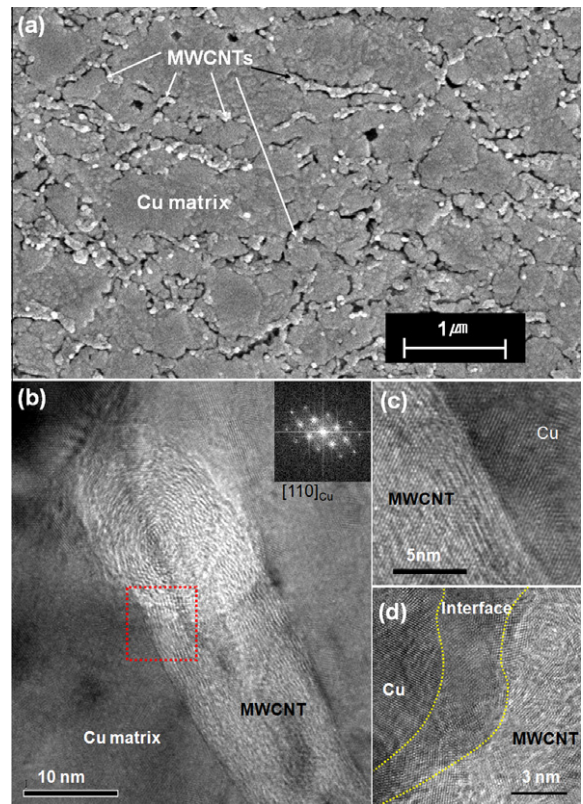
Figure 1. (a) Cross-sectional SEM image of wet-etched 5 vol.% CNT/Cu nanocomposites. (b) HRTEM image of embedded CNTs in the Cu matrix. (c) HRTEM image near to the side wall of a CNT. (d) HRTEM image revealing the interfacial region between the end tip of the CNT and the Cu matrix.

and that there are no inclusions between the CNT side wall and the Cu matrix, as shown in Figure 1c. However, atomically disordered regions close to the end of the multi-walled CNTs are observed. This is shown in Figure 1d, which displays the interface region marked by the dashed square in Figure 1b at higher magnification. Based on our previous result [11], it is expected that this kind of region corresponds to the CNT/Cu interface consisting of interfacial oxygen atoms stemming from the fabrication process and Cu atoms.

Figure 2 shows the thermal properties of the CNT/Cu nanocomposites in comparison with unreinforced Cu without CNTs. The thermal conductivity of the 5 and 10 vol.% CNT/Cu nanocomposites are about 250 and 200 W m^{-1} K^{-1}, respectively, even if the temperature increases from 298 to 550 K, as shown in Figure 2a. The CTE of the nanocomposites is distinctly lower than 17 ppm K^{-1} for unreinforced Cu for all investigated temperatures (Fig. 2b). Averaged CTEs of 14 and 12.1 ppm K^{-1} were obtained for the 5 and 10 vol.% CNT/Cu composites, respectively. The CTE values of the nanocomposites are closely related to enhanced stiffness [10,11], depending on the attractive force between the atoms. Thus, highly stiffened 10 vol.% CNT/Cu nanocomposites show the lowest CTE values compared to Cu.

The thermal conductivity variation as a function of CNT volume fraction at room temperature was normalized as K_c/K_m, where K_c is the thermal conductivity of

Table 1. Comparison of oxygen contents in the unreinforced Cu and CNT/Cu nanocomposite.

	Unreinforced Cu	5 vol.% CNT/Cu nanocomposite	10 vol.% CNT/Cu nanocomposite
Measured oxygen contents (wt.%)	0.25 ± 0.03	0.42 ± 0.05	0.55 ± 0.05
Excessive oxygen contents (wt.%)	–	0.17	0.30
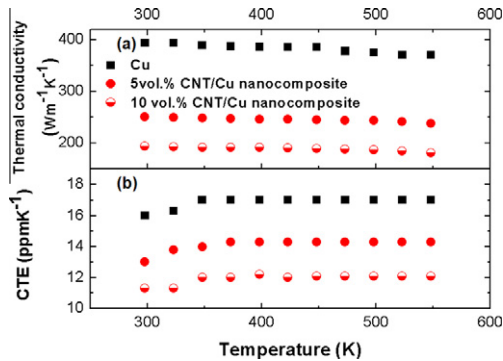
Figure 2. Thermal properties of CNT/Cu nanocomposites: (a) thermal conductivity with increasing temperature from 298 to 550 K; (b) variation of CTE compared with unreinforced Cu.

the CNT/Cu nanocomposites and K_m is the thermal conductivity of unreinforced Cu.

The measured K_c values are much lower than that of unreinforced Cu, as shown in Figure 3a. These results indicate that the embedded CNTs forming an intermediate interface, enabling effective load transfer between matrix and CNTs, do not act as a good thermally conductive region but rather as a thermal barrier, resulting in degradation of the overall thermal conductivity. We speculate that the low K_c is due to the large interface area formed by the functionalized CNTs that causes se-
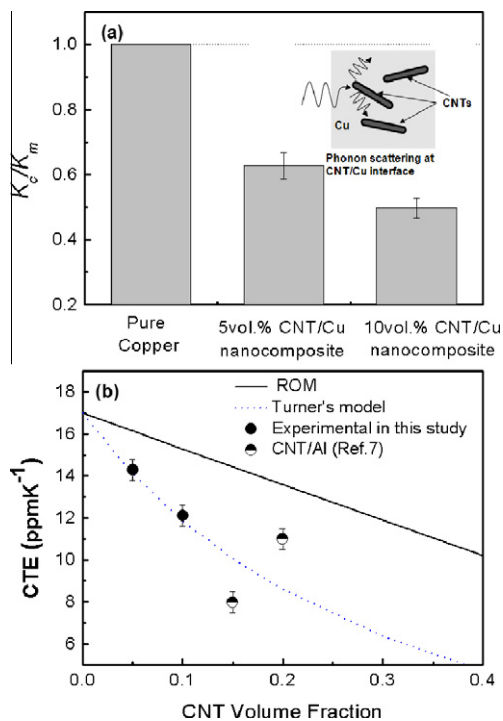
Figure 3. (a) Comparison of the normalized thermal conductivities of CNT/Cu nanocomposites with unreinforced Cu. (b) Comparison of the measured CTE with the calculated lines with CNT volume fraction.

vere lattice phonon dissipation, resulting in degradation of the thermal conductivity, very similar to the effect of nanoinclusions in thermoelectric materials [13].

On the other hand, the effect of the volume fraction of dispersed CNTs on the CTE of the composites can be estimated by the rule of mixtures and Turner's model [14], considering the constraint due to the difference in a dimensional change of each component by heating. The solid line and the dotted line in Figure 3b are the theoretically calculated values of the CTE with varying volume fraction of CNTs based on the rule of mixture and Turner's model, respectively. The experimentally determined CTE values agree well with the theoretical values based on Turner's model as the lower boundary in Figure 3b. From the viewpoint of electronic packaging materials demanding low CTE, it is worth noting that the CTE of CNT/Cu nanocomposites can be effectively reduced by adding more CNTs, as indicated by the values for CNT/Al composites taken from the literature [7]; these are also shown in Figure 3b for comparison.

These findings reveal that the thermal conductivity and the CTE of the nanocomposites depend closely on the CNT volume fraction, and embedded CNTs generating a strong interface should be treated as a key factor in controlling the thermal properties. Follow-up work is needed to clarify some critical issues when considering the use of CNT/Cu nanocomposites as electronic packaging materials: (1) the microstructure of composites with respect to the dispersion status of CNTs in the metal matrix; and (2) improved interface control for obtaining a high thermal conductivity. Despite these open issues, the current results reveal that the application of a metal matrix for CNT composites provides a good means to obtain a low CTE and even good thermal conductivity, as in the case of CNT/polymer composites [15].

In summary, CNT/Cu nanocomposites were fabricated by using the molecular-level mixing process, followed by spark plasma sintering. The resulting thermal properties show that CNT/metal nanocomposites in which CNTs are homogeneously embedded in the metal matrix are promising candidates for reducing CTE but require further interfacial treatment to obtain high thermal conductivity.

[1] P.K. Schebling, P. Keblinski, Phys. Rev. B. 68 (2003) 035425.
[2] S. Berber, Y.K. Kwon, D. Tomanek, Phys. Rev. Lett. 84 (2000) 4613.

[3] P. Kim, L. Shi, A. Majumdar, P.L. McEuen, Phys. Rev. Lett. 87 (2001) 215502.

[4] H. Huang, C. Liu, Y. Wu, S. Fan, Adv. Mater. (Weinheim, Ger.) 17 (2005) 1651.

[5] M.B. Bryning, D.E. Milkie, M.F. Islam, J.M. Kikkawa, A.G. Yoh, Appl. Phys. Lett. 87 (2005) 161909.

[6] A. Yu, M.E. Itkis, E. Bekyarova, R.C. Haddon, Appl. Phys. Lett. 89 (2006) 133102.

[7] Y. Tang, H. Cong, R. Zhong, H. Cheng, Carbon 42 (2004) 3251.

[8] N. Ferrer-Anglada, V. Gomis, Z. El-Hachemi, U.D. Weglikovska, M. Kaempgen, S. Roth, Phys. Status Solidi A 203 (2006) 1082.

[9] K. Chu, Q. Nu, C. Jia, X. Liang, J. Nie, W. Tian, G. Gai, H. Guo, Comput. Sci. Tech. 70 (2010) 298.

[10] S.I. Cha, K.T. Kim, S.N. Arshad, C.B. Mo, S.H. Hong, Adv. Mater. (Weinheim, Ger.) 17 (2005) 1377.

[11] K.T. Kim, S.I. Cha, T. Gemming, J. Eckert, S.H. Hong, Small 4 (2008) 1936.

[12] K.T. Kim, J. Eckert, S.B. Menzel, T. Gemming, S.H. Hong, Appl. Phys. Lett. 92 (2008) 121901.

[13] L.-D. Zhao, B. Zhang, J. Li, M. Zhou, W. Liu, J. Alloys Compd. 455 (2008) 259.

[14] P.S. Turner, J. Res. Nat. Bureau Standards USA 37 (1946) 239.

[15] S. Wang, Z. Liang, P. Gonnet, Y. Liao, B. Wang, C. Zhang, Adv. Funct. Mater. 17 (2007) 87.